


Article

# Full-Stokes, Multi-Frequency Radio Polarimetry of Fermi Blazars; Monitoring and Modelling

Emmanouil Angelakis \* , Ioannis Myserlis and J. Anton Zensus

Max Planck Institute for Radio Astronomy, 53121 Bonn, Germany; imyserlis@mpifr-bonn.mpg.de (I.M.); azensus@mpifr-bonn.mpg.de (J.A.Z.)

\* Correspondence: eangelakis@mpifr-bonn.mpg.de; Tel.: +49-228-525-217

Received: 31 August 2017; Accepted: 15 November 2017; Published: 20 November 2017

**Abstract:** The polarised emission from active galactic nuclei (AGN) jets carries information about the physical conditions at the emitting plasma elements, while its temporal evolution probes the physical processes that introduce variability and dynamically modify the local conditions. Here we present the analysis of multi-frequency radio linear and circular polarisation datasets with the aim of exactly quantifying the conditions in blazar jets. Our analysis includes both the careful treatment of observational datasets and numerical modelling for the reproduction of synthetic polarisation curves that can be compared to the observed ones. In our approach, the variability is attributed to traveling shocks. The emission from the cells of our jet model is computed with radiative transfer of all Stokes parameters. The model also accounts for Faraday effects which map the low-energy particle populations. We present two extreme cases in terms of the significance of Faraday conversion in the production of circular polarisation. As we show, in both regimes the model gives a realistic reproduction of the observed emission.

**Keywords:** AGN; jets; polarisation; linear; circular; radio; polarised radiative transfer

---

## 1. Introduction

The low-density relativistic plasma outflowing in the magnetised jet environment of active galactic nuclei (AGN) is responsible for the broadband synchrotron component that extends from radio to optical, UV, and often even X-ray photon energies (e.g., [1]). This component is often thought to be the *photon field* necessary for the operation of inverse Compton processes that energise photons even up to GeV energies or beyond.

For the subset of AGN with small jet viewing angle (the *blazars*), the intrinsically polarised synchrotron jet emission dominates the radio bands. Characterised by extreme phenomenologies, synchrotron emission is likely produced by sequential spectral components, whose evolution is arguably associated with disturbances (e.g., internal shocks) that travel in the plasma outflow [2]. The shocks modify the local conditions (particle density, magnetic field configuration, particle energies, etc.) and introduce variability in the jet polarised emission. The variable polarisation then maps the dynamics of the physical conditions at the emission sites. Additionally, the transmission through birefringent material such as magnetised plasma can further modify the transmitted radiation (e.g., Faraday effects) so that the variable polarised emission probes even the large scale environment of the jet.

Motivated by the need to understand and quantify these physical processes, we have been studying the multi-frequency linearly and circularly polarised radio emission for selected blazars. Our study includes both the observational analysis and the numerical modelling of all the Stokes parameters. Here we present two study cases that occupy two extremes of the particle energy distributions. Our model relies on the full-Stokes radiative transfer and produces synthetic light curves for all polarisation parameters immediately comparable with the observations. In the

two cases discussed here, we explore the role of the Faraday effects under different low-energy particle populations.

## 2. The Dataset

The bulk of the dataset discussed here is the result of the *F-GAMMA* program [3] that ran from January 2007 until January 2015. It sampled the band from 2.64 to 142 GHz at 10 frequency steps using the Effelsberg 100-m and IRAM 30-m telescopes for a total of around 90 mostly *Fermi* detected blazars. The nominal sampling rate was around one measurement every month, with the effective rate slightly above that. Until the upgrade of the receiver system at IRAM in mid-2009, the 228.93 GHz band was also monitored. The APEX 12-m telescope provided rather occasional monitoring at 345 GHz for a subset of sources. In Table 1, we summarise indicative characteristics of the used receivers as well as the data availability. Details on the observations, data reduction, and post-measurement data analysis for the total flux density are discussed extensively in [3,4].

**Table 1.** The receivers and the data availability for all observing frequencies. CP: circular polarisation; FWHM: full width at half maximum; LP: linear polarisation; HLP/VLP: horizontal/vertical linear polarisation; LCP/RCP: left/right-hand circular polarisation.

Frequency (GHz)	Bandpass (GHz)	Tsys (K)	FWHM (arcsec)	Polarisation Channels	Data Availability
<b>Effelsberg 100-m</b>					
2.64/10.45	0.1/0.3	17/52	260/68	LCP, RCP	LP: 2007–2011, 2014–2015: to be reduced ready LP: 2011–2014, 2015–now: to be reduced ready
4.85/8.35	0.5/1.2	27/22	146/82	LCP, RCP	CP: 2007–now: to be reduced ready LP: 2007–2010.5: to be reduced ready LP: 2010.5–now: to be reduced ready CP: 2007–2010.5: to be reduced ready CP: 2010.5–now: to be reduced ready
14.60	2.0	50	50	LCP, RCP	LP: 2007–now: to be reduced ready CP: 2007–now: to be reduced ready
23.05	2.7	77	36	LCP, RCP	LP: not available CP: 2007–now: to be reduced ready
32.00	4.0	64	25	LCP, LCP	LP, CP: not available
42.00	2.8	120	20	LCP, RCP	LP, CP: not available
<b>IRAM 30-m</b>					
86.24	1.0	~65	29	HLP, VLP	LP, CP: available elsewhere
142.33	1.0	~65	16	HLP, VLP	LP, CP: available elsewhere
228.93	1.0	~80	11	HLP, VLP	LP, CP: available elsewhere
<b>APEX 12-m</b>					
345.00	4.0	~100	~20		LP, CP: not available

As it is discussed in detail by [5,6], before any further analysis, the observed datasets are input to a data reduction pipeline that accounts for *instrumental linear* and *circular* polarisation (LP and CP) as well as other instrumental effects. The resulting accuracy—in terms of linear and circular polarisation degree—is of the order of 0.1–0.2 percent. The determination of the electric vector position angle (EVPA) is uncertain at a level of a few degrees. It is this careful treatment of instrumental effects that allows us the reliable reconstruction of all polarisation parameters—especially circular polarisation, which is intrinsically limited to challengingly low levels.

Starting in middle 2015 and only for the Effelsberg frequency range (2.64–43 GHz), we initiated a new program for the fast cadence monitoring of a limited sample of sources with a nominal cadence of two weeks. Table 2 lists the sources currently monitored with the scope to investigate the temporal evolution of their multi-frequency polarisation parameters and hence study the evolution of the polarised emitting plasma elements.

**Table 2.** The currently observed sources.

ID	Survey Name	Right Ascension (hh:mm:ss)	Declination (dd:mm:ss)	Remarks
J0324 + 3410	1H 0323 + 342	03:24:41.20	+34:10:45	NLSy1
J0841 + 7053	4C + 71.07	08:41:24.38	+70:53:41	
J0849 + 5108	SBS 0846 + 513	08:49:57.97	+51:08:29	NLSy1
J0854 + 2006	OJ 287	08:54:48.9	+20:06:31	
J0948 + 0022	PMN J0948 + 0022	09:48:57.32	+00:22:25	NLSy1
J1130 – 1449	PKS 1127 – 14	11:30:07.05	–14:49:27	
J1222 + 0413	SDSS J122222.55 + 041315.7	12:22:22.50	+04:13:16	NLSy1
J1229 + 0203	3C 273	12:29:06.70	+02:03:08	
J1256 – 0547	3C 279	12:56:11.17	–05:47:21	
J1443 + 4725	B3 1441 + 476	14:43:18.50	+47:25:57	NLSy1
J1505 + 0326	PKS 1502 + 036	15:05:06.50	+03:26:31	NLSy1
J1512 – 0905	PKS 1510 – 089	15:12:50.53	–09:05:59	
J1642 + 3948	3C 345	16:42:58.80	+39:48:37	
J1644 + 2619	FBQS J1644 + 2619	16:44:42.50	+26:19:13	NLSy1
J2202 + 4216	BL Lacertae	22:02:43.28	+42:16:40	
J2229 – 0832	PKS 2227 – 088	22:29:40.08	–08:32:54	
J2232 + 1143	CTA 102	22:32:36.40	+11:43:51	
J2253 + 1608	3C 454.3	22:53:57.74	+16:08:53	

### 3. The Jet Model

The variability observed in blazars is attributed to repeated episodes of intense activity that undergo spectral evolution [7] and are possibly caused by shocks traveling in the jet [2]. For modelling the variable emission and the dynamics of the polarisation parameters—both linear and circular—we assume that:

- the jet is magnetised with a partially uniform magnetic field.
- Occasional disturbances travel downstream in the flow, creating shocks that modify the local conditions by compressing the plasma and the local magnetic field.
- The particles at the shocked areas get re-energised and radiate flaring emission which undergoes spectral evolution.

In our model, the jet is made of *cells*, each one characterised by (a) a dominant uniform magnetic field component, (b) a much weaker turbulent one, and (c) homogeneous relativistic plasma populating a single power law energy distribution. The emission from each cell is treated in terms of all four Stokes parameters  $I$ ,  $Q$ ,  $U$ , and  $V$ . The degree of the *large-scale* magnetic field uniformity is implemented through the relative orientation of the field in individual cells. A propagating disturbance—a shock with a compression factor  $k$ —locally alters the particle density, the low energy cutoff  $\gamma_{\min}$ , and the magnetic field configuration, temporarily increasing its local uniformity. The evolution of the physical conditions imprints a certain evolution to the observed spectrum. The total radiation is computed by integrating over the entire extent of the jet after solving the full-Stokes radiative transfer problem along the line of sight, following the approach of [8,9]. During the radiation transport, all secondary effects are accounted for, so that the polarised emission intrinsic to the synchrotron mechanism is subjected to Faraday Rotation and Faraday Conversion. For the comparison with the data, synthetic total flux and polarisation light curves are produced by sampling the full-Stokes evolving spectra at our observing frequencies.

### 4. Results

#### 4.1. 3C 454.3: the High $\gamma_{\min}$ Regime

In Figure 1 we show all the polarisation parameters of 3C 454.3 as a function of time. In [6] we presented 3C 454.3 as a case for which our model reproduced synthetic light curves that were imitating the observed behaviour. More specifically, we found that assuming

- the presence of a random and a weak uniform magnetic field component; the magnetic induction of the uniform field is 5% of that of the random one,
- the magnetic induction of the random component at the base of the jet is 5 mG,
- magnetic field coherence length of  $\sim 9$  pc,
- plasma particle density  $n_0$  roughly in the range  $10\text{--}100\text{ cm}^{-3}$ ,
- the low particle energy cutoff  $\gamma_{\min} = 10^4$ ,
- a mild shock with compression factors  $k \sim 0.8$ , and
- Doppler factor of  $\sim 30$ ,

we were able to reproduce the temporal behaviour of the total flux density, the degree of linear and circular polarisation  $m_l$  and  $m_c$ , and the EVPA. The comparison of the synthetic and the observed light curves are shown in Figure 1 of [6]. This set of parameters proved able to produce what we assumed to be a the double opacity-driven flip of EVPA at MJD 55,500 and 56,500. The idea that these events are caused by transitions from optically thin and thick states of the emitting plasma and vice versa was supported by an associated nulling in the linear polarisation, the reversal of the circular polarisation handedness, and the maximisation of the total flux density. A scenario with a spectral component evolving in time within our bandpass and transitioning between thick and thin states would result in exactly this behaviour. This scenario is of course also evident in the evolution of the radio spectral energy distribution (SED). In fact, the SED behaviour indicates a sequence of similar components operating sequentially, creating a much richer phenomenology as time progresses.

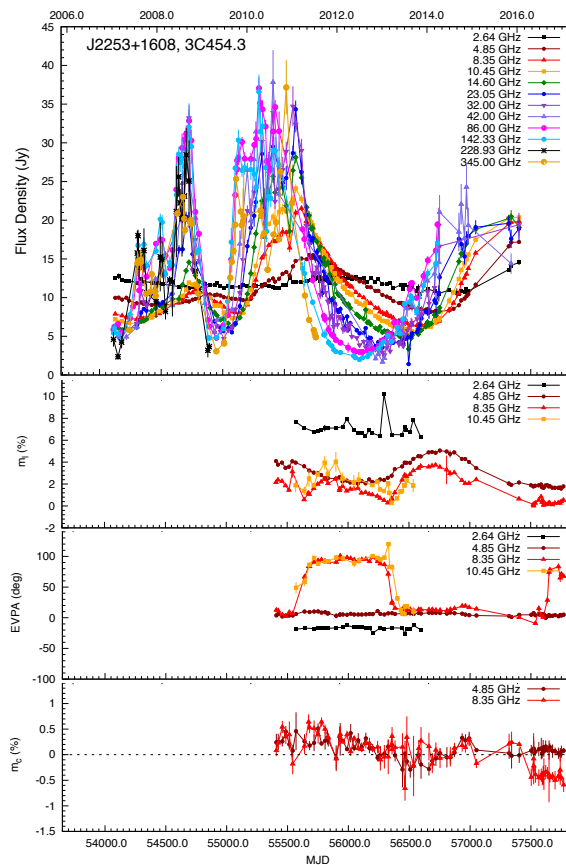


**Figure 1.** The polarisation state of the prototype source 3C 454.3 as a function of time. *From top to bottom:* The total flux density at all available frequencies, the degree of linear polarisation at four frequencies, the electric vector position angle (EVPA) at the same frequencies, and finally the degree of circular polarisation at 4.85 and 8.35 GHz.

#### 4.2. NGC 4845: The Low- $\gamma_{\min}$ Regime

For 3C 454.3,  $\gamma_{\min}$  was set to  $10^4$ . This implies that there is practically no low-energy particle population, which is necessary for the Faraday conversion of LP to CP. The modelled CP is therefore believed to be intrinsic to synchrotron mechanism and not induced by Faraday conversion. Irwin et al. [10] found that NGC 4845 was showing an evolving convex radio spectrum with a peak around 3–5 GHz. The linear polarisation of the source at both 1.5 GHz and 6 GHz was very low (0.1–0.5%), while the circular polarization at 1.5 GHz displayed unusually large values of around 2–3%. However, the CP was zero at 5 GHz.

We investigated the production of such large values of CP through the conversion of linear to circular polarisation. Indeed, the introduction of a significant low-energy particle population in the model— $\gamma_{\min} \sim 10$ –100—caused the transformation of LP to CP at 1.5 GHz, therefore attributing the low LP and high CP degrees to Faraday conversion. However, this setup could not explain the minimization of LP at 6 GHz. It is possible that at this frequency an excess of low-energy magnetized plasma within or around the flow may be causing depolarisation through Faraday rotation. In any case, it is necessary to further investigate this assumption by including such an excess component in the model.

As a conclusion, also in the low- $\gamma_{\min}$  regime our adopted jet model gives very realistic reconstruction of the observed behaviour.

### 5. Discussion and Conclusions

In the previous, we presented an end-to-end polarisation data analysis that aims at utilising the multi-frequency monitoring of linear and circular polarisation in order to quantify the physical conditions and processes at plasma emission elements in blazar jets. Our analysis includes not only the careful data treatment that allows the recovery of reliable polarisation datasets, but also the theoretical modelling of the emission. The radio variability in blazar jets is assumed to be caused by shocks that induce a spectrally evolving emission as they propagate down the stream. Our model relies on a full Stokes radiative transfer, and treats all major transmission effects formally. In both low- and high- $\gamma_{\min}$  regimes, where the Faraday effects are important or suppressed, respectively, the model produces polarisation light curves that reproduce the observed behaviour exactly. In the former case, the assumption of an excess population of low-energy particles to explain the linear de-polarisation at 6 GHz seems to be needed.

**Acknowledgments:** This research is based on observations with the 100-m telescope of the MPIfR (Max-Planck-Institut für Radioastronomie) at Effelsberg. The authors thank the MPIfR internal referee B. Boccardi for the useful comments.

**Author Contributions:** E.A. and I.M. conceived and designed the project; I.M. developed the model and did all the analysis. I.M. and E.A. performed the observations and analysed the data; J.A.Z. contributed in the discussion and the interpretation of the data; E.A. wrote the paper.

**Conflicts of Interest:** The authors declare no conflict of interest.

### Abbreviations

The following abbreviations are used in this manuscript:

LP/CP	Linear/Circular Polarisation
LCP/RCP	Left/Right-hand Circular Polarisation (referring to channel)
HLP/VLP	Horizontal/Vertical Linear Polarisation (referring to channel)
NLSy1	Narrow Line Seyfert 1
EVPA	Electric Vector Position Angle

## References

1. Begelman, M.C.; Blandford, R.D.; Rees, M.J. Theory of extragalactic radio sources. *Rev. Mod. Phys.* **1984**, *56*, 255–351.
2. Marscher, A.P.; Gear, W.K. Models for high-frequency radio outbursts in extragalactic sources, with application to the early 1983 millimeter-to-infrared flare of 3C 273. *Astrophys. J.* **1985**, *298*, 114–127.
3. Fuhrmann, L.; Angelakis, E.; Zensus, J.A.; Nestoras, I.; Marchili, N.; Pavlidou, V.; Karamanavis, V.; Ungerechts, H.; Krichbaum, T.P.; Larsson, S.; et al. The F-GAMMA programme: Multi-frequency study of active galactic nuclei in the Fermi era. Programme description and the first 2.5 years of monitoring. *Astron. Astrophys.* **2016**, *596*, A45.
4. Angelakis, E.; Fuhrmann, L.; Marchili, N.; Foschini, L.; Myserlis, I.; Karamanavis, V.; Komossa, S.; Blinov, D.; Krichbaum, T.P.; Sievers, A.; et al. Radio jet emission from GeV-emitting narrow-line Seyfert 1 galaxies. *Astron. Astrophys.* **2015**, *575*, A55.
5. Myserlis, I.; Angelakis, E.; Kraus, A.; Liontas, C.A.; Marchili, N.; Aller, M.F.; Aller, H.D.; Karamanavis, V.; Fuhrmann, L.; Krichbaum, T.P.; et al. Full-Stokes polarimetry with circularly polarized feeds—Sources with stable linear and circular polarization in the GHz regime. *arXiv* **2017**, arXiv:1706.04200.
6. Myserlis, I.; Angelakis, E.; Kraus, A.; Fuhrmann, L.; Karamanavis, V.; Zensus, J. Physical Conditions and Variability Processes in AGN Jets through Multi-Frequency Linear and Circular Radio Polarization Monitoring. *Galaxies* **2016**, *4*, 58.
7. Angelakis, E.; Fuhrmann, L.; Nestoras, I.; Fromm, C.M.; Perucho-Pla, M.; Schmidt, R.; Zensus, J.A.; Marchili, N.; Krichbaum, T.P.; Ungerechts, H.; et al. F-GAMMA: On the phenomenological classification of continuum radio spectra variability patterns of Fermi blazars. *J. Phys. Conf. Ser.* **2012**, *372*, doi:10.1088/1742-6596/372/1/012007.
8. Jones, T.W.; Odell, S.L. Transfer of polarized radiation in self-absorbed synchrotron sources. I—Results for a homogeneous source. *Astrophys. J.* **1977**, *214*, 522–539.
9. Hughes, P.A.; Aller, H.D.; Aller, M.F. Synchrotron emission from shocked relativistic jets. I—The theory of radio-wavelength variability and its relation to superluminal motion. *Astrophys. J.* **1989**, *341*, 54–79.
10. Irwin, J.A.; Henriksen, R.N.; Krause, M.; Wang, Q.D.; Wiegert, T.; Murphy, E.J.; Heald, G.; Perlman, E. CHANG-ES V: Nuclear Outflow in a Virgo Cluster Spiral after a Tidal Disruption Event. *Astrophys. J.* **2015**, *809*, 172.



© 2017 by the authors. Licensee MDPI, Basel, Switzerland. This article is an open access article distributed under the terms and conditions of the Creative Commons Attribution (CC BY) license (<http://creativecommons.org/licenses/by/4.0/>).